

CD44 Mediated Nonviral Gene Delivery into Human Embryonic Stem Cells via Hyaluronic-Acid-Coated Nanoparticles

Jonathan Yen,^{†,§} Hanze Ying,[‡] Hua Wang,[‡] Lichen Yin,[⊥] Fatih Uckun,^{||,¶} and Jianjun Cheng^{*,‡,†}

[†]Department of Bioengineering and [‡]Department of Materials Science and Engineering, University of Illinois at Urbana–Champaign, Urbana, Illinois 61801, United States

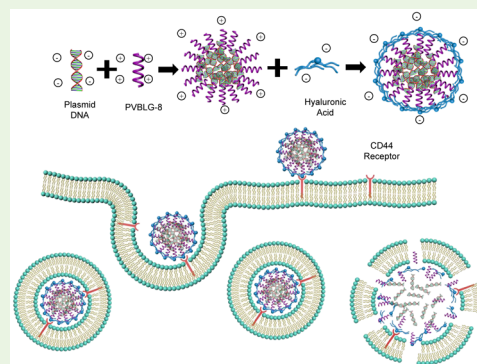
[⊥]Jiangsu Key Laboratory for Carbon-Based Functional Materials & Devices, Institute of Functional Nano & Soft Materials, Collaborative Innovation Center of Suzhou, Nano Science and Technology, Soochow University, Suzhou 215123, PRC

^{||}Developmental Therapeutics Program, Children's Hospital Los Angeles, Children's Center for Cancer and Blood Diseases, Los Angeles, California 90027, United States

[¶]Department of Pediatrics and Norris Comprehensive Cancer Center, University of Southern California Keck School of Medicine, Los Angeles, California 90027, United States

ABSTRACT: Gene delivery is an important tool to study and manipulate human pluripotent stem cells for regenerative medicine purposes. Yet current methods of transient gene delivery to stem cells are still inefficient. Through the combination of biologically based concepts and material design, we aim to develop new methods to enhance the efficiency of gene delivery to stem cells. Specifically, we use poly(γ -4-(((2-(piperidin-1-yl)ethyl)amino)methyl)benzyl-L-glutamate) (PVBLG-8), a membrane-active helical, cationic polypeptide, to condense plasmid DNA to form stable nanocomplexes, which are further coated with hyaluronic acid (HA). HA not only shields the positive charges of PVBLG-8 to reduce toxicity, but also acts as a targeting moiety for cell surface receptor CD44, which binds HA and facilitates the internalization of the nanocomplexes. Upon entering cells, HA is degraded by hyaluronidase in endosomes and PVBLG-8 is exposed, facilitating the endosomal escape of DNA/polypeptide complex. Our studies show that the coating of HA significantly increases gene transfection efficiency of DNA/PVBLG-8 nanocomplexes from about 28 to 36% with largely reduced toxicity.

KEYWORDS: human embryonic stem cells, nonviral gene delivery, polypeptides, human pluripotent stem cells, hyaluronic acid, CD44



1. INTRODUCTION

Human embryonic stem cells (hESCs) hold tremendous potential in the field of regeneration due in particular to two characteristics: pluripotency and self-renewal. In pursuit of regenerative medicine, gene delivery is an important tool to manipulate and control cell fate. The control and overexpression of specific genes afforded by gene delivery is valuable not only in efforts to control stem cell fate^{1–4} and for gene targeting studies.^{5,6} Currently, viral gene delivery is still the tool of choice for gene overexpression in hESCs for mechanistic and differentiation studies, due to its high transfection efficiency and stable transgene expression.⁷ But viral gene delivery is plagued with issues that are unsuitable for biomedical applications, including random viral integration into the host, high cytotoxicity, immunogenicity, and insertional mutagenesis.^{8,9} Nonviral gene delivery has gradually become an important tool for stem cell engineering to transiently express genes of interest with reduced toxicity, providing a promising alternative to viral gene delivery.^{10–16}

There have been various materials developed for nonviral gene delivery into a variety of cells such as poly beta amino

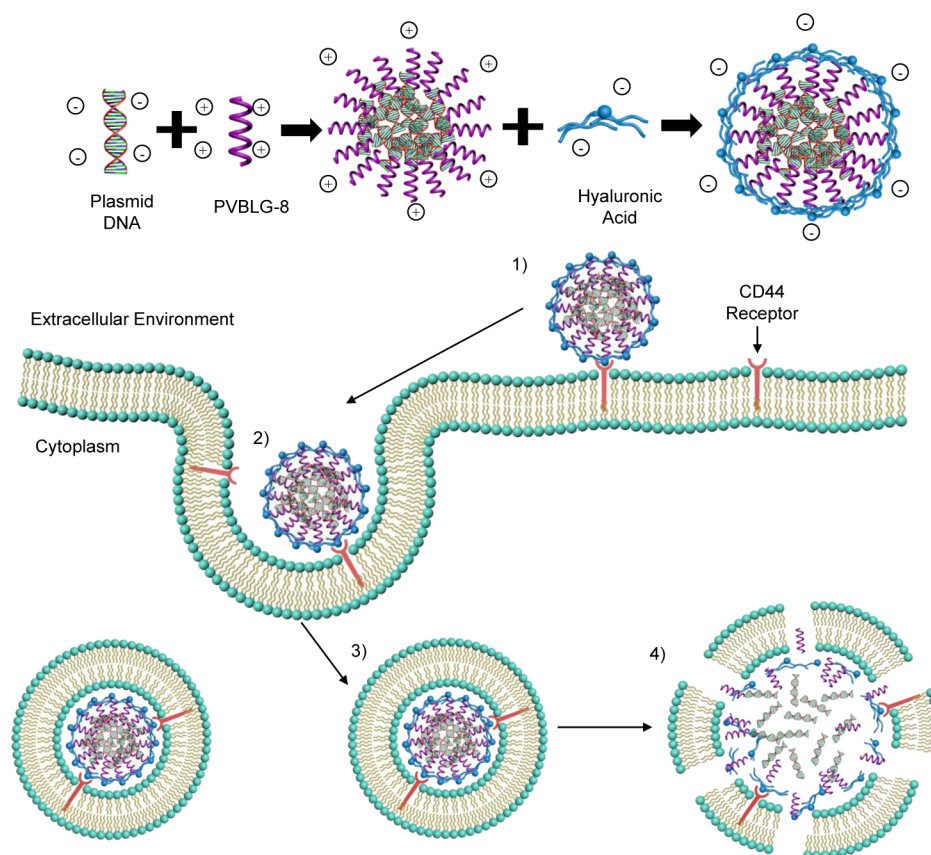
esters¹⁷ and helical polypeptides.^{18,19} However, many issues remain to be addressed in nonviral gene delivery, particularly in hESCs, such as low transfection efficiency and high cytotoxicity. Because of the physiology of hESCs, nonviral gene delivery to hESCs usually has low uptake efficiency.^{17,20} We have reported that commonly used nonviral gene delivery materials including PEGylated PVBLG-8, polylysine (PLL), polyethylenimine, and commercially available Lipofectamine 2000 demonstrates transfection efficiencies of 8, 3, 8, and 10% in hESCs, respectively.^{18,20} Green group's poly beta amino esters demonstrated transfection efficiency of 15–20%.¹⁷ Efforts have been made to improve the cell uptake of nanoparticles by modifying their surface with certain targeting ligands that can specifically bind to cell surface protein receptors.^{21–26} After entering cells, the DNA/plasmids need to reach the nucleus for transcription, which instead are usually trapped in the endosomes and thus tagged for degradation. We thus aimed

Received: September 11, 2015

Accepted: January 26, 2016

Published: February 23, 2016

Scheme 1. Formulation and Uptake Route of the Hyaluronic-Acid-Coated PVBLG-8/DNA Nanocomplexes; (1) HA-Coated Nanocomplexes Target and Bind to CD44 Receptors; (2) Nanocomplexes are Uptaken through Receptor-Mediated Endocytosis; (3) Low pH and Hyaluronidase Break down Nanocomplexes within Endosomes; (4) PVBLG-8 Peptides Break through Endosome Membranes and Allow Cargo to Escape



to develop an effective delivery system with active targeting motif coated on the complex, which not only can enhance the uptake of the gene delivery vehicles and shield the cationic polymers to reduce cytotoxicity, but can also quickly escape from endosome after rapid dissociation of the charged shielding moiety in the endosome.

Poly(γ -4-(((2-(piperidin-1-yl)ethyl)amino)methyl)benzyl-L-glutamate) (PVBLG-8), a novel helical, charged polypeptide developed in our group, has been demonstrated to possess excellent membrane disruption and endosomal escape capability as a gene delivery system,^{27–42} which can be attributed to the cationic charge and rigid α -helical structure.^{19,37,43} Although PVBLG-8 shows some gene transfection efficiency in hESCs, it exhibits typical charge-associated cytotoxicity to the cells.¹⁹ Our lab has developed multiple methods to modify the cationic helical polypeptide to reduce its toxicity, such as structural reconfiguration,²⁹ conjugations,^{18,28,31} and incorporation of trigger-degradable protection group,³² while retaining or increasing its transfection efficiency through enhanced endosomal escape capability. Herein, we report a new gene delivery system based on self-assembled DNA/PVBLG-8 nanocomplexes coated with negatively charged hyaluronic acid (HA). HA can specifically bind to CD44, a known cell surface receptor with high expression level in hESCs.⁴⁴ By coating the DNA/PVBLG-8 nanocomplexes with negatively charged HA, it not only shields the positive charges of PVBLG-8 to decrease the toxicity of nanocomplexes, but also acts as a targeting moiety for receptor based endocytosis through HA/CD44 interactions

in hESCs, enhancing cellular uptake. Furthermore, the HA can be deshielded by endogenous hyaluronidase in endosomes after cellular internalization to expose the membrane-active cationic helical PVBLG-8, allowing rapid and efficient endosomal release and expression of DNA plasmids (Scheme 1). We expect the new design will lead to higher hESC transfection efficiency and lower cytotoxicity.

2. MATERIALS AND METHODS

2.1. General. hESCs H1 (hESC-H1) was cultured in E8 medium from Stem Cell Technologies (Vancouver, Canada). Human mesenchymal stem cells (hMSCs) were purchased from Lonza (Basel, Switzerland). COS-7 cells were purchased from ATCC (Manassas, VA, USA). Y-27632 was purchased from Stemgent (Cambridge, MA, USA). YOYO-1 was purchased from Invitrogen (Carlsbad, CA, USA). pEGFP-N1 was obtained from Elim Biopharmaceuticals (Hayward, CA, USA). Milli-Mark Anti-SSEA-4-PE was purchased from EMD Millipore (Billerica, MA, USA). PVBLG-8, a helical cationic polypeptide with a degree of polymerization of 200, was synthesized following previously reported procedures.⁴⁵

2.2. Instrumentation. Flow cytometry analysis was conducted on a BD LSRII flow cytometry analyzer (Becton Dickinson, Franklin Lakes, NJ). Cells were visualized with a Zeiss Axiovert 40 CFL fluorescence microscope equipped with 10 and 20x objectives (Thornwood, NY). Zeta potential and size analysis was conducted on the Malvern Zetasizer (Worcestershire, UK).

2.3. Nanocomplex Formation and Characterization. Various nonviral vectors were used for the transfection analyses. Plasmid DNA (1 μ L, 1 mg/mL) was diluted in water (25 μ L). PVBLG-8 (7.5 μ L, 1

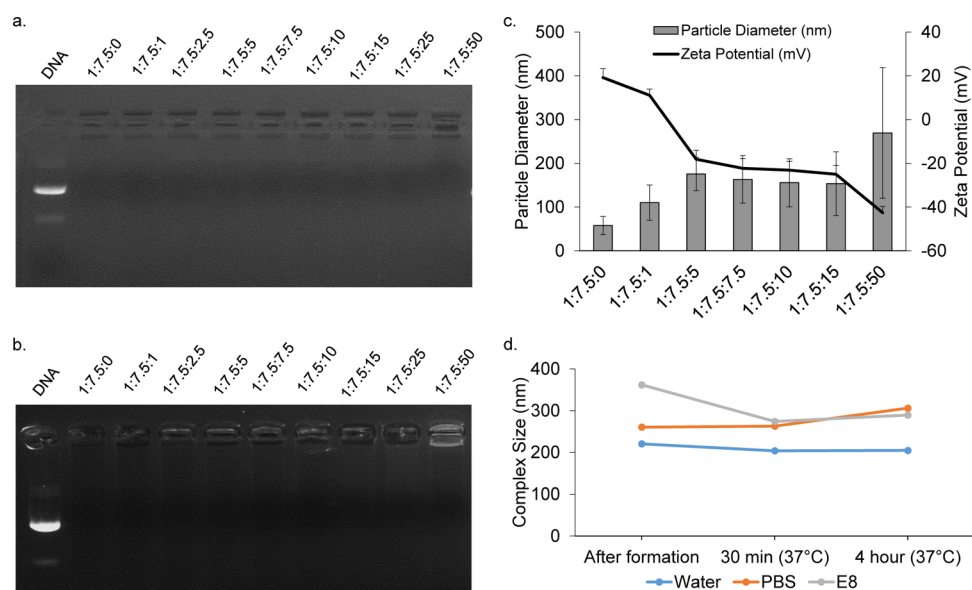


Figure 1. Characterization of HA-coated nanocomplexes at 1:7.5 DNA:PVBLG-8 weight ratios (a) Gel retardation of varying HA-coated nanocomplexes. (b) Gel retardation of a HA mixed with DNA nanocomplexes at 1:7.5:7.5. (c) Size and zeta potential of HA coated nanocomplexes. (d) Stability of HA coated nanocomplexes (1:7.5:7.5) in water, PBS, and E8 medium as determined by size change measured by DLS.

mg/mL) was diluted with water (25 μ L). For the PVBLG-8 and coated nanocomplex procedures, the PVBLG-8 and plasmids were mixed at various ratios and were incubated for 20 min at rt for complex formation. Hyaluronic acid (2.5–50 μ L, 1 mg/mL) in water was added to the nanocomplex mixture and incubated for another 20 min at rt. For the mixed system, the DNA and hyaluronic acid were first mixed together at various ratios and then PVBLG-8 was added. The mixture was incubated at rt for 30 min for complex formation. Dynamic light scattering (DLS) and zeta potential analysis were conducted on the samples with a Malvern Zetasizer (Worcestershire, UK). The nanocomplexes were subjected to electrophoresis in 1% agarose gel at 100 V for 45 min to evaluate DNA condensation by the polypeptides in terms of DNA migration.

2.4. In Vitro Gene Transfection. Cells were seeded in matrigel coated 24 well plates as single cells using accutase and incubated for 24 h with rho-kinase inhibitor Y-27632 (10 μ M). Using fresh low protein and serum free E8 medium, nanocomplexes as described earlier were added at 1 μ g DNA/well. After incubation for 4 h, the medium was replaced with fresh E8 medium and cells were cultured for 48 h. The cells were collected with accutase, fixed with paraformaldehyde and analyzed using flow cytometry to determine transfection efficiency.

2.5. In Vitro HA Blocking. hESCs were incubated with free hyaluronic acid (300 kDa, 1–5 mg/mL) for 1 h prior to transfection. The cells were then washed 1x with PBS and placed back with fresh E8 media. The nanocomplexes were added to the cells at 1 μ g DNA/well. After incubation for 4 h, the medium was replaced with fresh E8 medium and cells were cultured for 48 h. The cells were collected with accutase, fixed with paraformaldehyde and analyzed using flow cytometry to determine transfection efficiency.

2.6. pH and Hyaluronidase Exposure of Nanocomplex. Nanocomplexes were formulated as previous described. HA coated nanocomplexes (400 μ L, 100 μ g/mL DNA) were incubated with hyaluronidase (100 μ L, 0.5 mg/mL) in phosphate and citric acid buffer with a pH of 7.4, 6.8, 6.2, or 5.6 for 0, 30, or 120 min at 37 $^{\circ}$ C. The HA coated nanocomplexes (100 μ L) were then diluted in their corresponding buffer and the zeta potential of the resulting particles was analyzed with the Zetasizer.

To test the membrane activity of the nanocomplexes, we formulated large unilamellar vesicles by extrusion technique (LUVETS)⁴⁶ loaded with 8-aminonaphthalene-1,3,6-trisulfonic acid (ANTS) and *p*-xylene-bis-pyridinium bromide (DPX).⁴⁷ Briefly, DOPC (100 μ L, 25 mg/mL CHCl_3) and POPC (1 mL, 10 mg/mL CHCl_3) were mixed in round-bottom flask and evaporated with a rotary evaporator to create dry thin

film. The film was allowed to dry overnight under vacuum. The lipid film was rehydrated by 5 mL of ANTS/DPX solution (12.5 mM ANTS, 45 mM DPX, 10 mM phosphate buffer, pH 7.4) for 30 min at rt. The solution was then put through 5 freeze thaw cycles in liquid nitrogen and lukewarm water. The solution was then extruded 15 times through 0.4 μ M polycarbonate membranes. Any extravesicular components were removed through a Sephadex G-50 gel filtration column.

Nanocomplexes were formulated as previous described. HA coated nanocomplexes (400 μ L, 100 μ g/mL DNA) were incubated with hyaluronidase (100 μ L, 0.5 mg/mL) in phosphate and citric acid buffer at pH 7.4 or 6.8 for 0 or 30 min at 37 $^{\circ}$ C. The HA coated nanocomplexes (10 μ L) and the ANTS/DPX LUVETS (5 μ L) were mixed and diluted by the corresponding buffer to a final solution of 100 μ L. Triton x was used as the positive control. The leaked ANTS dye was measured using a plate reader at 360 nm excitation and 530 nm emission. The final leakage percentage was calculated using the ratio of fluorescence of the sample with the positive control after background subtraction.

2.7. Cell Viability. Cells were seeded in matrigel coated 96 well plates as single cells using accutase and incubated for 24 h with y-27632 (10 μ M). Using fresh low protein and serum free E8 medium, nanocomplexes were added at 0.2 μ g DNA/well. After incubation for 4 h, the medium was replaced with fresh E8 medium and cells were cultured for 48 h. Cell viability was evaluated through a MTT assay. Cells without complex treatment served as the control and results were expressed as percentage viability of control cells.

2.8. Intracellular Uptake Studies. DNA (1 mg/mL) was mixed and labeled with YOYO-1 (20 μ M) at one dye molecule per 50 bp of DNA. The HA coated nanocomplexes were then formed with YOYO-1/DNA as discussed before at a DNA:PVBLG-8:HA weight ratio of 1:7.5:7.5. hESCs were plated on matrigel coated 24-well plate and allowed to grow to medium sized colonies. The complexes were added to the wells at 1 μ g of YOYO-1-DNA per well and incubated for 4 h at 37 $^{\circ}$ C. The cells were then quantified through flow cytometry to quantify YOYO-1 uptake. Results are expressed as mean fluorescence levels.

To elucidate the mechanisms regarding the cellular internalization of DNA/PVBLG-8/HA complexes, we performed the uptake study at 4 $^{\circ}$ C or in the presence of various endocytic inhibitors for 2 h. Cells were pretreated with chlorpromazine (10 μ g/mL), genistein (200 μ g/mL), dynasore (80 μ M), and wortmannin (50 nm) for 30 min before the complexes were added and throughout the experiment for 2 h at

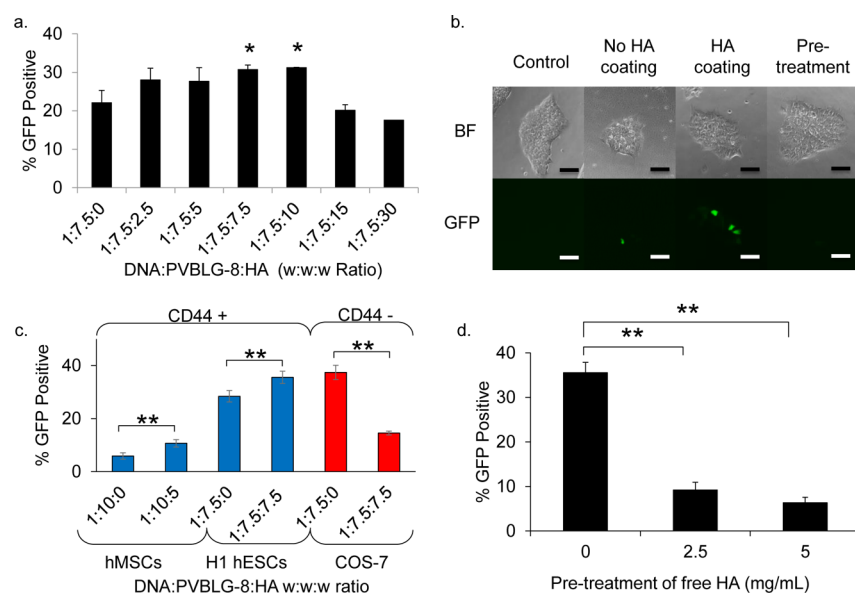


Figure 2. HA-coated nanocomplexes significantly enhance the transfection efficiency of GFP encoding plasmid in hESCs. (a) Flow cytometry analysis of transfection efficiency of hESCs with varying ratios of HA coating on DNA:PVBLG-8 nanocomplexes. (One-way ANOVA analysis with Dunnett's post-testing with 1:7.5:0 as control, $n = 3$ * $p < 0.05$ error bars: Std. Dev.) (b) Fluorescence images of H1 hESCs 48 h post transfection with and without HA coated nanocomplexes and with 5 mg/mL free HA pretreatment (scale bar = 250 μm). (c) Flow cytometry analysis of transfection comparison between CD44(+) hMSCs and hESCs, and CD44(-) COS-7 cells to demonstrate the effect of HA targeting. (t test comparison $n = 3$ * $p < 0.05$ ** $p < 0.01$, error bars: Std. Dev.) (d) Transfection of 1:7.5:7.5 nanocomplexes in cells pretreated with 0, 2.5, or 5 mg/mL of free HA. (t test comparison $n = 3$ * $p < 0.05$ ** $p < 0.01$, error bars: std. dev.)

37 °C. Results are expressed as percentage of the mean GFP fluorescence level at 37 °C in control cells in the absence of endocytic inhibitors.

2.9. Western Blot Analysis and SSEA Staining. After 72 h of transfection, the cells were stained with DAPI (250 μL , 3 nM) and SSEA-4-PE (250 μL , 0.02 mg/mL), a pluripotency cell marker, for 30 min at 37 °C. After 5 d, the cells were collected with RIPA buffer and mixed with Laemmli buffer supplemented with 2-mercaptoethanol, heated at 100 °C for 5 min to denature the proteins and then put on ice. The samples were ran on 10% SDS PAGE Gel at 120 V for 1.5 h, and wet transferred to the nitrocellulose membrane using the AMRESCO Rapid Western Blot Kit per manufacturer's instructions. The membrane was stained with OCT4 and α -Tubulin primary antibodies and then with HRP-tagged secondaries.

2.10. Statistical Analysis. All statistics analysis were performed by GraphPad Prism v6.07. Multiple group comparisons were analyzed using one-way ANOVA analysis with Dunnett's post-testing with 1:7.5:0 as control, $n = 3$, and with significance of $p < 0.05$. Significance between two groups were performed by student t test, $n = 3$, and with significance of $p < 0.05$ and $p < 0.01$.

3. RESULTS

3.1. Characterization of DNA:PVBLG-8:HA Nanocomplexes. DNA condensation by PVBLG-8 followed by HA coating, through charge interaction of the negatively charged HA and the positively charged PVBLG-8, was evaluated by gel retardation assay. As shown in Figure 1a, DNA can be bound tightly to PVBLG-8 with a weight feeding ratio of 1:7.5. Coating of HA on the nanocomplex did not disrupt or displace the DNA in the nanocomplexes at the feeding ratio of DNA to PVBLG-8 to HA ranging from 1:7.5:0 to 1:7.5:50. These results indicate that the complexes are stable through the coating, and the negative charges on the HA does not interfere in the assembly stability and does not lead to disassembly of the nanocomplexes. Yet, when the HA was mixed directly with the DNA and PVBLG-8, the complex was unstable and some DNA leakage was detected (Figure 1b), substantiating the importance

of performing DNA/PVBLG-8 complex prior to the coating with HA.

The size and zeta potential of the DNA/PVBLG-8 nanocomplexes at 1:7.5 weight ratios with varying HA weight ratio coatings were characterized using the DLS and zetasizer (Figure 1c). Without HA coating, the nanocomplex size was 57.9 nm in diameter. After the coating of HA, at between 1:7.5:5 and 1:7.5:15 weight ratios, the effective diameters increased to and stabilized around 170 nm. With further addition of HA to 1:7.5:50, the diameter increased to 270 nm with an additional peak at 5.1 μm (data not shown), suggesting substantial change of the morphology and aggregation of the nanocomplex and presumably weakened interaction of DNA/PVBLG-8, although leakage of DNA was not observed. This observation also clearly showed the dynamic interaction of HA with the nanocomplex. The zeta potential of the nanocomplex without HA, measured to be 19.2 mV, decreased to 11.1 mV with HA coating at 1:7.5:1 ratio, indicating that the nanocomplexes retained their positive charges with surface partially covered by HA. The zeta potential then decreases to between -18 and -25 mV when the ratio of DNA:PVBLG-8:HA was between 1:7.5:5 and 1:7.5:15, and to -42 mV at DNA:PVBLG-8:HA ratio of 1:7.5:50. The increase of the size and decrease of zeta potential suggest that formation of nanocomplexes with HA coating can be achieved via a dynamic process and the amount of HA on nanocomplex surface can be modulated by the amount HA added, but materials and charge balance are critical to the intended functions nanocomplexes and should impact their gene delivery efficiency to cells. HA with transient stability on the nanocomplex surface enhances uptake, contributes to the desired dissociation of HA from the nanocomplexes upon internalization into the endosomes, and exposes PVBLG-8 for endosomal release.

The stability of the nanocomplexes at the optimal DNA:PVBLG-8:HA ratio (1:7.5:7.5) was selected due to the

highest transfection efficiency in hESCs (see Figure 2a) and tested in water, PBS and E8 medium through the use of the dynamic light scattering to determine the size of the nanocomplexes over time under various conditions (Figure 1d). The particle stability was tested for up to 4 h (typical incubation time for transfection) after formulation at 37 °C. We assumed that if the HA coating was unstable, the size of the nanocomplex would likely increase due to charge-induced aggregation. Experimental results showed that the sizes of nanocomplex remained constant in different media over time, which indicated that the nanocomplexes are quite stable.

3.2. hESC Transfection with HA-Coated DNA/PVBLG-8 Nanocomplexes. Through the optimization of various DNA:PVBLG-8 weight ratios, 1:7.5 was found to be the optimal ratio that gave the highest transfection efficiency (data not shown). Thus, the DNA:PVBLG-8 ratio was fixed at 1:7.5 with various ratios of HA coating on the nanocomplexes. Without HA coating, the nanocomplexes achieved 22% transfection efficiency, while with the increasing ratio of HA coated on the nanocomplexes, the transfection efficiency went up to 28%, 27% and 30% for 7.5:2.5, 7.5:5, 7.5:7.5 of PVBLG-8:HA ratios, respectively. As we increased the amount of HA to 15 and 30, the transfection efficiency decreased to 20 and 17%, respectively (Figure 2a, b). The decrease in transfection efficiency might be attributed to the excess HA in the system that does not coat the nanocomplexes but competes for the binding with CD44 receptors. PVBLG-8 by itself showed medium toxic to the cells (Figure 3a). With HA coating, nanocomplexes showed reduced toxicity and higher transfection.

To demonstrate that the targeting of the HA coated nanocomplexes were due to the CD44 binding of the HA coated on the surface, pretreatment of free HA was applied to the cells for 30 min and then washed off before transfection. With the pretreatment of 2.5 and 5 mg/mL of free HA, a drop of transfections to 8 and 6% were shown, respectively (Figure 2d). This indicates that free HA bound to the cell surface CD44 receptors block the uptake of nanocomplex, suggesting CD44-mediated uptake of the nanocomplex. To further demonstrate the importance of the CD44 receptor for the system, the HA coated nanocomplexes were transfected in CD44 positive human mesenchymal stem cells (hMSCs) and CD44 negative COS-7 cells (Figure 2c). For CD44 positive hMSCs, HA coated nanocomplexes showed almost twice the transfection efficiency than that without HA coating. In contrast, in CD44 negative COS-7 cells, the transfection efficiency was 36% without the HA coating and it dropped down to 15% after HA coating (Figure 2d), which was probably due to the negative charge of HA shielding the nanocomplexes. These trends demonstrates the important roles the CD44 receptors play in the transfection, which may be due to the increased uptake of the HA-coated nanocomplexes.

3.3. Toxicity and Maintenance of hESCs. Cytotoxicity of the HA coated complexes was evaluated in hESCs 48 h after transfection using the MTT assay. PVBLG-8 demonstrated a cell viability of 75% (Figure 3a). But with the HA coated nanocomplexes, the cell viability increased to approximately 90% with the HA coated at 1:7.5:7.5 weight ratios (Figure 3a). To ensure that the materials did not alter the cell's behavior or cause any differentiation, we stained the cells with SSEA-4 antibodies, stage specific embryonic antigen-4, 72 h after transfection, in which the cells all stained positive (Figure 3b). In addition, cell lysate were collected 5 days after transfection

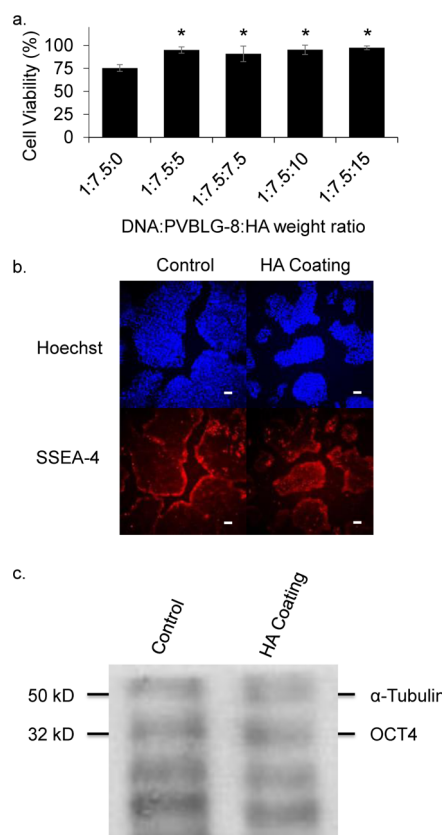


Figure 3. HA-coated nanocomplexes do not compromise pluripotency and reduces cell toxicity. (a) Cell viability of hESCs at varying ratios of HA coating of nanocomplexes as determined by MTT assay. (One-way ANOVA analysis with Dunnett's post-testing with 1:7.5:0 as control, $n = 3$, * $p < 0.05$) b) DAPI and SSEA4 staining patterns of hESCs 72 h after transfected with HA coated nanocomplexes (scale bar = 250 μm). (c) Western blot analysis shows OCT4 expression in hESCs 5 days post HA-coated nanocomplexes transfection, the bottom two bands are nonspecific.

and a Western blot was conducted to confirm the continued expression of the pluripotent factor, OCT4 (Figure 3c). The expression of SSEA-4 and OCT4 demonstrated that this system does not cause undesired differentiation or interferes with the pluripotency of the hESCs.

3.4. Mechanistic Studies of DNA/PVBLG-8/HA Nanocomplexes. To demonstrate that the enhanced gene transfection is due to the increased uptake through the CD44 receptor mediated pathway, the total uptake of DNA was evaluated. Using DNA tagged with YOYO-1, the amount of DNA/YOYO-1 uptake into the cells was determined. From Figure 4, it can be seen that without HA coating, the mean YOYO-1 fluorescence level measured to be about 61%, whereas with the HA coating at 1:7.5:7.5 ratio, the mean YOYO-1 fluorescence increased to 67%. In addition, with the treatment of free HA, the mean YOYO-1 fluorescence level decline significantly to around 44%, indicating a reduced nanocomplex uptake. Alternatively, the uptake of DNA/YOYO-1 in CD44 negative COS-7 cells is reduced significantly after the coating of HA, further demonstrating that the CD44 receptor mediated the uptake of HA coated nanocomplexes (Figure 4c).

To demonstrate that the HA coated nanocomplexes were indeed targeting the CD44 receptors, hESCs were stained with CD44 antibodies and incubated with HA-coated DNA/YOYO-1/PVBLG-8 nanocomplexes for 2 h at 4 °C. Through confocal

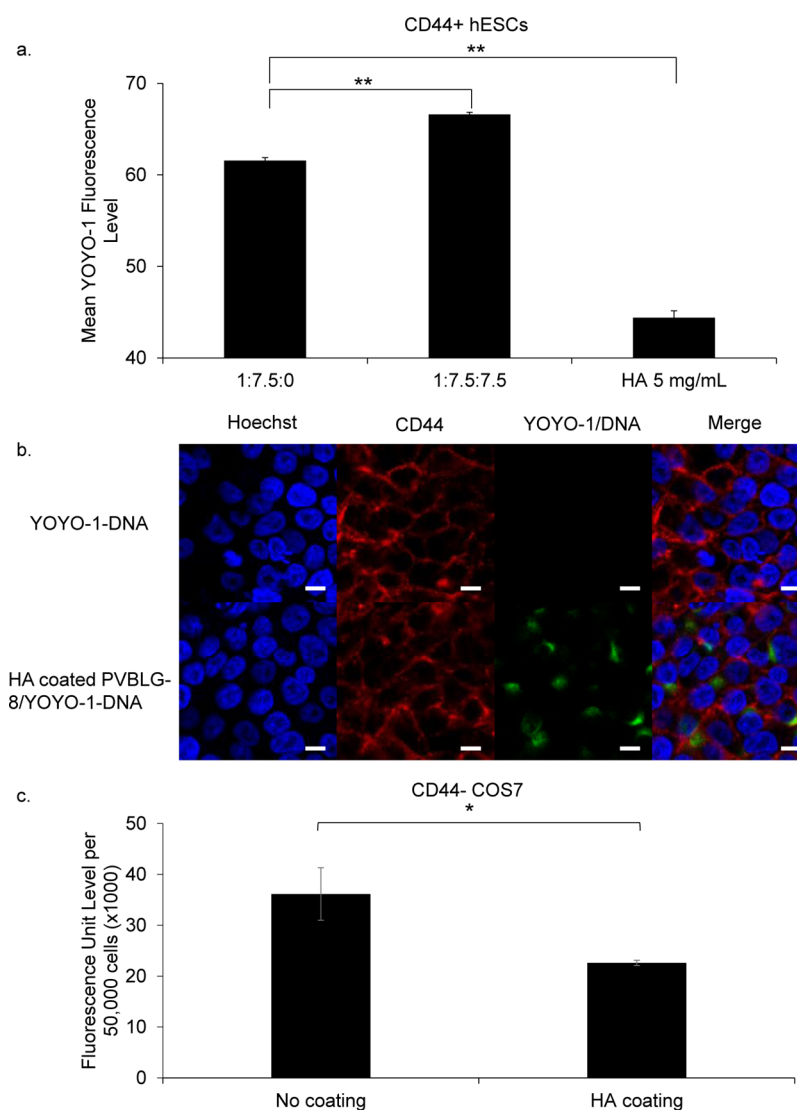


Figure 4. HA-coated nanocomplexes promotes cellular internalization of the gene cargo through CD44 receptor interactions. (a) Cell uptake level of PVBLG-8/YOYO-1-DNA complexes in hESCs with varying amounts of HA coating and with the pretreatment of hESCs with free HA ($n = 3$). (b) CLSM images of hESCs incubated with HA coated PVBLG-8/YOYO-1-DNA complexes at 4 °C for 1 h with CD44-PE antibody staining (scale bar = 10 μ m). (c) Cell uptake level of YOYO-1-DNA/PVBLG-8 complexes with and without HA coating in CD44 negative COS-7 cells at 1:7.5 weight ratios. (*t* test comparison $n = 3$ * $p < 0.05$ ** $p < 0.01$, error bars: std. dev.).

imaging, CD44 is stained uniformly across the surface of the hESCs. The DNA/YOYO-1 can be visualized on the cell surface colocalized with the CD44 receptors, indicating the importance of the roles of the CD44/HA interactions (Figure 4b).

To elucidate the mechanisms underlying the cellular internalization of the HA-coated nanocomplexes, we performed the uptake study at 4 °C or in the presence of various endocytic inhibitors. Energy-dependent endocytosis was blocked at 4 °C; clathrin-mediated endocytosis was blocked by chlorpromazine, which triggers dissociation of the clathrin lattice; caveolae was inhibited by genistein and m β CD by inhibiting tyrosine kinase and depleting cholesterol, respectively; macropinocytosis was inhibited by wortmannin by inhibiting phosphatidylinositol-3-phosphate.^{48,49} When the cells were incubated at 4 °C, the uptake dropped to almost 3% of the control, whereas chlorpromazine dropped to 62%, genistein dropped to 22%, and wortmannin to 91% of the control (Figure 5a). The dramatic decrease of transfection efficiency at 4 °C indicates the

process is energy dependent, and with the decrease of uptake with the treatment of chlorpromazine and genistein, further demonstrates that the nanocomplexes enter the cells through receptor mediated endocytosis.

Because of the high membrane disruption ability of PVBLG-8, the YOYO-1-DNA can quickly escape the endosomes and permeate into the cell cytoplasm after 2 h incubation at 37 °C (Figure 5b). PLL, a substitute cationic peptide with lower membrane disruption ability was used to visualize the uptake and localization of the HA coated complexes. Through confocal imaging, there is significant colocalization of the HA coated YOYO-1-DNA/PLL complex with the LysoTracker red stain as seen through CLSM confocal imaging (Figure 5b). It demonstrates that HA coating facilitates the nanocomplex uptake through receptor mediated endosomal pathway. But it also showed that PVBLG-8 nanocomplex induces more efficient endosomal escape, which is beneficial for gene transfection.¹⁹ We demonstrated that PVBLG-8 is exposed from the nanocomplex through HA degradation to allow for

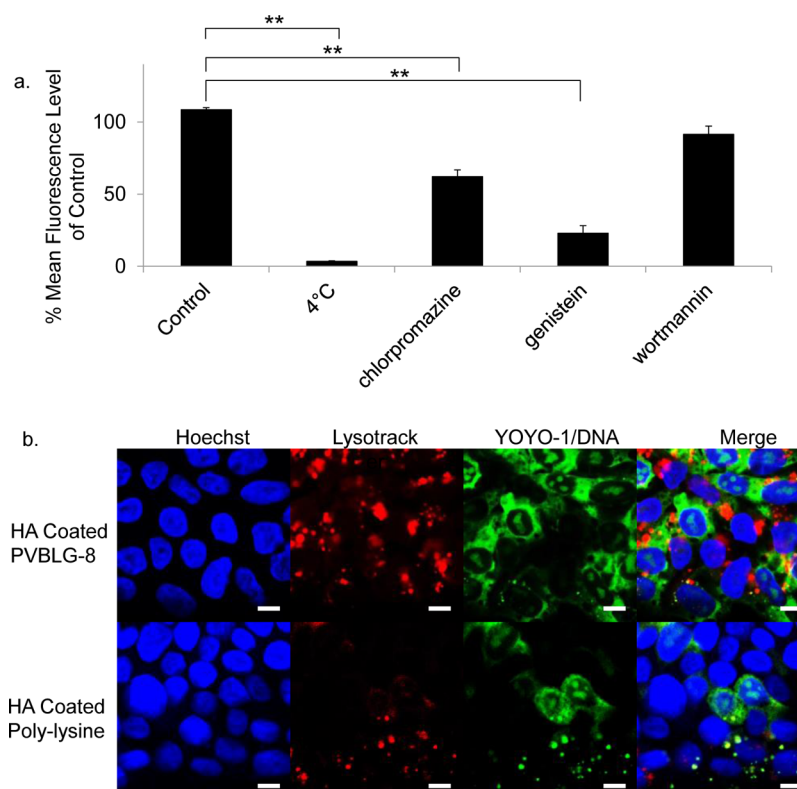


Figure 5. HA-coated nanocomplexes promotes cellular internalization of the gene cargo through endocytosis. (a) Cell uptake mechanisms of HA coated PVBLG-8/YOYO-1-DNA complexes in hESCs. ($n = 3$). (b) CLSM images of uptake and endosomal escape of HA-coated PVBLG-8/YOYO-1-DNA and PLL/YOYO-1-DNA complexes and with Lysotracker staining (scale bar = 10 μm) (t test comparison $n = 3$ ** $p < 0.01$, error bars: std. dev.).

membrane disruption and endosomal escape once the nanocomplex reaches the endosomes in the following studies.

3.5. Exposure of PVBLG-8 from HA-Coated Nanocomplex for Endosomal Escape. The rapid endosomal escape of the nanocomplex was presumably due to PVBLG-8 exposure as the HA coating is released and digested in the endosomal environment. To investigate the mechanism of endosome triggered membrane disruption of HA-coated nanocomplexes for rapid endosomal escape, we evaluated the nanocomplex zeta potentials and membrane disruption abilities after treatment with hyaluronidase (HAase) at varying endosomal pH. At the initial time point of incubation of the HAase with varying pH of 7.4, 6.8, 6.2 and 5.6, the zeta potential remains negative at -21 , -17.6 , -16.8 , and -10.3 mV, respectively. After 30 min incubation, the zeta potential at pH of 7.4 and 6.8 increased but remained negative at -18.2 and -8.32 mV, respectively. On the other hand, the zeta potential at pH of 6.2, and 5.6, all increased to the positive range of 1.34 and 9.39 mV, respectively. Finally, after 120 min the zeta potential at pH of 7.4 stays negative at -9.3 mV. But, for the pH at 6.8, 6.2 and 5.6, the zeta potential increases to positive of 1.69, 7.2, and 11.8 mV, respectively. A pH of 7.4 is representative of the cytoplasmic pH, whereas early and late endosomes have a pH of 6.8 and 5.6, respectively⁵⁰ (Figure 6a). The shift of zeta potential toward positive indicates the exposure of the cationic helical peptides, which are then capable of membrane disruption.

To further illustrate that the membrane disruption ability of the HA-coated nanocomplexes at an early pH endosome of 6.8 is due to the HAase degradation rather than pH-induced complex dissociation, large unilamellar vesicles (LUV) were

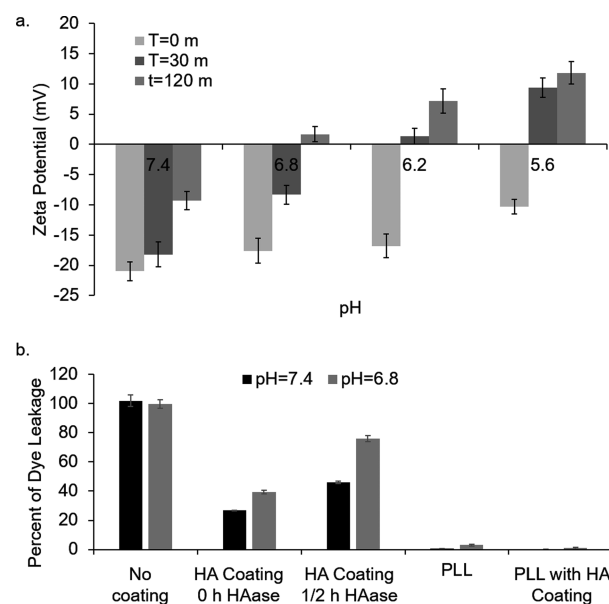


Figure 6. pH and HAase effect on HA-coated nanocomplexes. (a) Changes in the zeta potential of DNA/PVBLG-8/HA nanocomplexes after treatment with 0.5 mg/mL of HAase at different pH values for different times. (b) ANTS/DPX-loaded LUVET leakage study of different nanocomplexes with and without the HAase treatment at different pH values.

synthesized for dye leakage assay. At a pH of 7.4 and 6.8, it can be seen that the non-HA-coated nanocomplexes allowed for 100% release of the dye, whereas with HA coating, the

nanocomplexes only demonstrated slight membrane disruption at pH of 7.4, and a slight increase in membrane disruption at a pH of 6.8. Alternatively, with the addition of HAase after 30 min incubation at pH of 7.4 and 6.8, the dye leakage increased up to 46% and 76%, respectively, indicating strong membrane disruption ability (Figure 6b). In addition, nanocomplexes using PLL were also studied and it was found that with or without HA coating, there was no membrane disruption as expected. These studies indicated that the HA coated PVBLG-8 nanocomplex is responsive to the endosomal environment with enhanced HAase activity induced by low pH, allowing for rapid endosomal escape with the exposed PVBLG-8.

4. DISCUSSION

We developed a novel gene transfection system that contains an outer negatively charged cell targeting shell consisting of HA, with an inner core made from a cationic helical peptide capable of condensing DNA and facilitating endosomal escape. The system utilizes the charge interactions between the outer negatively charged shell and positive inner core to stabilize the nanocomplex at neutral pH, but allows for the deshelling and exposure of the positive helical peptides when exposed to a lower pH and HAase within the endosome. With the HA coating of the nanocomplexes, the hESC transfection efficiency of DNA/PVBLG-8 nanocomplexes increases significantly, despite the alteration of the overall surface charge from positive to negative. HA coated nanocomplexes also lower the toxicity of the cationic helical peptide and have little effect on the cells pluripotency, for hESCs were still both OCT4 and SSEA4 positive after materials treatment. HA is a negatively charged biocompatible polysaccharide that is found naturally in the body and has been used as the backbone of many hydrogel systems for stem cell engineering.⁴⁴ A few glycosaminoglycans, except for hyaluronic acid have been shown to disrupt cationic polypeptide gene transfections.⁵¹ The reversal of charge indicates the loss of the initial membrane disruption effect of the cationic helical peptide, which in theory should have decreased transfection. However, this study showed that the negative nanocomplexes increased the transfection efficiency, indicating that the HA on the nanocomplexes are an integral part to the transfection efficiency, in which they target the CD44 receptors that are expressed on hESC surfaces. We found that at weight ratios of 1:7.5:0 to 1:7.5:7.5, the transfection efficiency increases, which then decreases with additional HA coating. This decrease is likely to be caused by the excess HA that was not coated on the nanocomplex. This can be seen by the DLS and zeta potential, that after a certain ratio, the size and zeta potential of the nanocomplex stays constant. Thus, the excess free HA could be competitively binding with the CD44 receptor against the nanocomplexes demonstrated by the drastic drop in transfection efficiency with the pretreatment of HA. The decrease in transfection efficiency demonstrated that the free HA has bound to the cell surface CD44 receptors and blocked them from further uptake, indicating that the CD44/HA interactions is an important aspect to the increased efficacy of the nanocomplex. The HA coated nanocomplexes also demonstrated a higher efficacy in CD44 positive hMSCs, but substantially reduced transfection efficiency in CD44 negative COS-7 cells, substantiating the importance of the CD44 receptor for the uptake of the HA coated nanocomplexes.

To understand the mechanism of uptake, we conducted uptake studies of DNA tagged with YOYO-1 dye and found that the cells did significantly increase the uptake of the

nanocomplexes with the HA coating. In addition, through the study with various endocytosis inhibitors, we found that at 4 °C the uptake was drastically inhibited, indicating that the uptake of the particles were highly energy dependent. In addition, the decrease of the uptake due to the chlorpromazine, demonstrated that some of the particles were internalized through clathrin-dependent endocytosis. On the other hand, genistein also had a large decrease in uptake of the YOYO-1/DNA, thus indicating that some of the uptake is due to clathrin independent pathways like caveolae mediated uptake. All these evidence showed that the materials were internalized through receptor mediated pathways.

Commonly used transfection materials like PLL have the ability to condense DNA for nonviral gene delivery, but PLL demonstrates no endosomal escape.^{52,53} Our nanocomplex system transforms to exhibit membrane disruptive properties in endosomal environment with high HAase activity induced by low pH. The exposure of PVBLG-8 in the system enhances the endosomal release of the nanocomplex and thus the DNA. When the materials were switched to PLL, a nonmembrane disrupting polymer, there was little endosomal escape, and the nanocomplexes were mainly retained in the endosomes. In early endosomes, at a low pH and some HAase activity, the HA coated nanocomplexes demonstrated increased LUV dye leakage due to membrane disruption. Our system is superior to other materials^{17,18,20} because of our highly available and active membrane disruption activity that is initially shielded to reduce cytotoxicity to the cells, but is revealed when it enters the endosomes. Thus, through the use of a targeting moiety for a receptor on hESCs is a step in looking at nonviral gene delivery into hESCs differently, in which a cell's specific mechanism is exploited to enhance transfection efficiency.

5. CONCLUSION

We reported a new targeting and triggerable gene delivery system for human embryonic stem cells based on the PVBLG-8, a cationic helical polypeptide with high membrane disruption properties. The DNA/PVBLG-8 nanocomplex by itself was demonstrated to be toxic to the cells because of the high membrane disruption properties. Using HA as a coating for the nanocomplexes not only decreased the toxicity from the cationic helical peptides, but also allowed targeting of hESCs and deshelling of charge shielding moiety that increased the uptake and release of DNA, which in turn increased the transfection efficiency. This provides a promising approach to manipulate hESCs or pluripotent stem cells through transient gene delivery, overcoming major hurdles toward development of various biomedical applications. Increased gene transfection efficiency reduces the need for enrichment and sorting of the manipulated pluripotent stem cells. These preliminary studies demonstrated an enhanced gene delivery system to undifferentiated hESCs through an alternate receptor-mediated endocytosis pathway and allows for future modification with other targeting moieties on the PVBLG-8 based gene delivery to target other receptors on other hard to transfect cells.

■ AUTHOR INFORMATION

Corresponding Author

*E-mail: jianjunc@illinois.edu. Tel: (217) 244-3924.

Present Address

§J.Y. is currently at NGx, Developmental and Molecular Pathways, Novartis Institutes for BioMedical Research, Cambridge, Massachusetts, 02139, USA

Author Contributions

The manuscript was written through contributions of all authors. All authors have given approval to the final version of the manuscript.

Notes

The authors declare no competing financial interest.

ACKNOWLEDGMENTS

This work is supported by NIH (Director's New Innovator Award 1DP2OD007246 and 1R21EB013379 for J.C.) for the biological studies of the project and NSF (CHE 1153122) for the synthesis and development of the polypeptide. J.Y. was funded at UIUC from National Science Foundation (NSF) Grant 0965918 IGERT: Training the Next Generation of Researchers in Cellular and Molecular Mechanics and BioNanotechnology.

REFERENCES

- (1) Reubinoff, B. E.; Pera, M. F.; Fong, C.-Y.; Trounson, A.; Bongso, A. Embryonic stem cell lines from human blastocysts: somatic differentiation in vitro. *Nat. Biotechnol.* **2000**, *18* (4), 399–404.
- (2) Cai, J.; Zhao, Y.; Liu, Y.; Ye, F.; Song, Z.; Qin, H.; Meng, S.; Chen, Y.; Zhou, R.; Song, X.; et al. Directed differentiation of human embryonic stem cells into functional hepatic cells. *Hepatology* **2007**, *45* (5), 1229–1239.
- (3) Zhang, Y.; Pak, C.; Han, Y.; Ahlenius, H.; Zhang, Z.; Chanda, S.; Marro, S.; Patzke, C.; Acuna, C.; Covy, J.; et al. Rapid Single-Step Induction of Functional Neurons from Human Pluripotent Stem Cells. *Neuron* **2013**, *78* (5), 785–798.
- (4) Gropp, M.; Itsykson, P.; Singer, O.; Ben-Hur, T.; Reinhartz, E.; Galun, E.; Reubinoff, B. E. Stable genetic modification of human embryonic stem cells by lentiviral vectors. *Mol. Ther.* **2003**, *7* (2), 281–287.
- (5) Zou, J.; Maeder, M. L.; Mali, P.; Pruetz-Miller, S. M.; Thibodeau-Beganny, S.; Chou, B. K.; Chen, G.; Ye, Z.; Park, I. H.; Daley, G. Q. Gene targeting of a disease-related gene in human induced pluripotent stem and embryonic stem cells. *Cell Stem Cell* **2009**, *5* (1), 97–110.
- (6) Mali, P.; Yang, L.; Esvelt, K. M.; Aach, J.; Guell, M.; DiCarlo, J. E.; Norville, J. E.; Church, G. M. RNA-guided human genome engineering via Cas9. *Science* **2013**, *339* (6121), 823–826.
- (7) Ye, Z.; Yu, X.; Cheng, L. Lentiviral gene transduction of mouse and human stem cells. *Methods Mol. Biol.* **2008**, *430*, 243–53.
- (8) Thomas, C. E.; Ehrhardt, A.; Kay, M. A. Progress and problems with the use of viral vectors for gene therapy. *Nat. Rev. Genet.* **2003**, *4* (5), 346–358.
- (9) Davé, U. P.; Jenkins, N. A.; Copeland, N. G. Gene therapy insertional mutagenesis insights. *Science* **2004**, *303* (5656), 333.
- (10) Leong, K.; Mao, H.; Roy, K.; Walsh, S.; August, J. DNA-polycation nanospheres as non-viral gene delivery vehicles. *J. Controlled Release* **1998**, *53* (1–3), 183.
- (11) Kizjakina, K.; Bryson, J. M.; Grandinetti, G.; Reineke, T. M. Cationic glycopolymers for the delivery of pDNA to human dermal fibroblasts and rat mesenchymal stem cells. *Biomaterials* **2012**, *33* (6), 1851–1862.
- (12) McLendon, P. M.; Fichter, K. M.; Reineke, T. M. Poly (glycoamidoamine) vehicles promote pDNA uptake through multiple routes and efficient gene expression via caveolae-mediated endocytosis. *Mol. Pharmaceutics* **2010**, *7* (3), 738–750.
- (13) Srinivasachari, S.; Reineke, T. M. Versatile supramolecular pDNA vehicles via “click polymerization” of β -cyclodextrin with oligoethyleneamines. *Biomaterials* **2009**, *30* (5), 928–938.

- (14) Yang, F.; Cho, S. W.; Son, S. M.; Bogatyrev, S. R.; Singh, D.; Green, J. J.; Mei, Y.; Park, S.; Bhang, S. H.; Kim, B. S.; et al. Genetic engineering of human stem cells for enhanced angiogenesis using biodegradable polymeric nanoparticles. *Proc. Natl. Acad. Sci. U. S. A.* **2010**, *107* (8), 3317–3322.

- (15) Yang, F.; Green, J.; Dinio, T.; Keung, L.; Cho, S.; Park, H.; Langer, R.; Anderson, D. Gene delivery to human adult and embryonic cell-derived stem cells using biodegradable nanoparticulate polymeric vectors. *Gene Ther.* **2009**, *16* (4), 533–546.

- (16) Shim, M. S.; Kwon, Y. J. Acid-transforming polypeptide micelles for targeted nonviral gene delivery. *Biomaterials* **2010**, *31* (12), 3404–3413.

- (17) Green, J. J.; Zhou, B. Y.; Mitalipova, M. M.; Beard, C.; Langer, R.; Jaenisch, R.; Anderson, D. G. Nanoparticles for gene transfer to human embryonic stem cell colonies. *Nano Lett.* **2008**, *8* (10), 3126–3130.

- (18) Yen, J.; Zhang, Y.; Gabrielson, N. P.; Yin, L.; Guan, L.; Chaudhury, I.; Lu, H.; Wang, F.; Cheng, J. Cationic, helical polypeptide-based gene delivery for IMR-90 fibroblasts and human embryonic stem cells. *Biomater. Sci.* **2013**, *1* (7), 719–727.

- (19) Gabrielson, N. P.; Lu, H.; Yin, L. C.; Li, D.; Wang, F.; Cheng, J. J. Reactive and Bioactive Cationic α -Helical Polypeptide Template for Nonviral Gene Delivery. *Angew. Chem., Int. Ed.* **2012**, *51* (5), 1143–1147.

- (20) Yen, J.; Yin, L.; Cheng, J. Enhanced non-viral gene delivery to human embryonic stem cells via small molecule-mediated transient alteration of the cell structure. *J. Mater. Chem. B* **2014**, *2* (46), 8098–8105.

- (21) Cho, H. J.; Yoon, H. Y.; Koo, H.; Ko, S. H.; Shim, J. S.; Lee, J. H.; Kim, K.; Kwon, I. C.; Kim, D. D. Self-assembled nanoparticles based on hyaluronic acid-ceramide (HA-CE) and Pluronic (R) for tumor-targeted delivery of docetaxel. *Biomaterials* **2011**, *32* (29), 7181–7190.

- (22) Cho, H. J.; Yoon, I. S.; Yoon, H. Y.; Koo, H.; Jin, Y. J.; Ko, S. H.; Shim, J. S.; Kim, K.; Kwon, I. C.; Kim, D. D. Polyethylene glycol-conjugated hyaluronic acid-ceramide self-assembled nanoparticles for targeted delivery of doxorubicin. *Biomaterials* **2012**, *33* (4), 1190–1200.

- (23) Choi, K. Y.; Chung, H.; Min, K. H.; Yoon, H. Y.; Kim, K.; Park, J. H.; Kwon, I. C.; Jeong, S. Y. Self-assembled hyaluronic acid nanoparticles for active tumor targeting. *Biomaterials* **2010**, *31* (1), 106–114.

- (24) Choi, K. Y.; Min, K. H.; Na, J. H.; Choi, K.; Kim, K.; Park, J. H.; Kwon, I. C.; Jeong, S. Y. Self-assembled hyaluronic acid nanoparticles as a potential drug carrier for cancer therapy: synthesis, characterization, and in vivo biodistribution. *J. Mater. Chem.* **2009**, *19* (24), 4102–4107.

- (25) Choi, K. Y.; Min, K. H.; Yoon, H. Y.; Kim, K.; Park, J. H.; Kwon, I. C.; Choi, K.; Jeong, S. Y. PEGylation of hyaluronic acid nanoparticles improves tumor targetability in vivo. *Biomaterials* **2011**, *32* (7), 1880–1889.

- (26) Kim, E. J.; Shim, G.; Kim, K.; Kwon, I. C.; Oh, Y. K.; Shim, C. K. Hyaluronic acid complexed to biodegradable poly L-arginine for targeted delivery of siRNAs. *J. Gene Med.* **2009**, *11* (9), 791–803.

- (27) Zheng, N.; Song, Z.; Liu, Y.; Zhang, R.; Zhang, R.; Yao, C.; Uckun, F. M.; Yin, L.; Cheng, J. Redox-responsive, reversibly-crosslinked thiolated cationic helical polypeptides for efficient siRNA encapsulation and delivery. *J. Controlled Release* **2015**, *205*, 231–239.

- (28) Zheng, N.; Yin, L. C.; Song, Z. Y.; Ma, L.; Tang, H. Y.; Gabrielson, N. P.; Lu, H.; Cheng, J. J. Maximizing gene delivery efficiencies of cationic helical polypeptides via balanced membrane penetration and cellular targeting. *Biomaterials* **2014**, *35* (4), 1302–1314.

- (29) Yin, L.; Song, Z.; Kim, K. H.; Zheng, N.; Tang, H.; Lu, H.; Gabrielson, N.; Cheng, J. Reconfiguring the architectures of cationic helical polypeptides to control non-viral gene delivery. *Biomaterials* **2013**, *34* (9), 2340–9.

- (30) Yin, L.; Song, Z.; Qu, Q.; Kim, K. H.; Zheng, N.; Yao, C.; Chaudhury, I.; Tang, H.; Gabrielson, N. P.; Uckun, F. M.; Cheng, J.

Supramolecular Self-Assembled Nanoparticles Mediate Oral Delivery of Therapeutic TNF- α siRNA against Systemic Inflammation. *Angew. Chem., Int. Ed.* **2013**, *52* (22), 5757–5761.

(31) Yin, L. C.; Song, Z. Y.; Kim, K. H.; Zheng, N.; Gabrielson, N. P.; Cheng, J. J. Non-Viral Gene Delivery via Membrane-Penetrating, Mannose-Targeting Supramolecular Self-Assembled Nanocomplexes. *Adv. Mater.* **2013**, *25* (22), 3063–3070.

(32) Yin, L. C.; Tang, H. Y.; Kim, K. H.; Zheng, N.; Song, Z. Y.; Gabrielson, N. P.; Lu, H.; Cheng, J. J. Light-Responsive Helical Polypeptides Capable of Reducing Toxicity and Unpacking DNA: Toward Nonviral Gene Delivery. *Angew. Chem., Int. Ed.* **2013**, *52* (35), 9182–9186.

(33) Yin, L. C.; Chen, Y. B.; Zhang, Z. H.; Yin, Q.; Zheng, N.; Cheng, J. J. Biodegradable Micelles Capable of Mannose-Mediated Targeted Drug Delivery to Cancer Cells. *Macromol. Rapid Commun.* **2015**, *36* (5), 483–489.

(34) Uckun, F. M.; Ma, H.; Cheng, J. J.; Myers, D. E.; Qazi, S. CD22DE12 as a molecular target for RNAi therapy. *Br. J. Haematol.* **2015**, *169* (3), 401–414.

(35) Torabi, S. F.; Wu, P. W.; McGhee, C. E.; Chen, L.; Hwang, K.; Zheng, N.; Cheng, J. J.; Lu, Y. In vitro selection of a sodium-specific DNAAzyme and its application in intracellular sensing. *Proc. Natl. Acad. Sci. U. S. A.* **2015**, *112* (19), 5903–5908.

(36) Zheng, C.; Niu, L.; Pan, W.; Zhou, J. H.; Lv, H.; Cheng, J. J.; Liang, D. H. Long-term kinetics of DNA interacting with polycations. *Polymer* **2014**, *55* (10), 2464–2471.

(37) Lu, H.; Wang, J.; Song, Z. Y.; Yin, L. C.; Zhang, Y. F.; Tang, H. Y.; Tu, C. L.; Lin, Y.; Cheng, J. J. Recent advances in amino acid N-carboxyanhydrides and synthetic polypeptides: chemistry, self-assembly and biological applications. *Chem. Commun.* **2014**, *50* (2), 139–155.

(38) Deng, X. J.; Zheng, N.; Song, Z. Y.; Yin, L. C.; Cheng, J. J. Trigger-responsive, fast-degradable poly(beta-amino ester)s for enhanced DNA unpacking and reduced toxicity. *Biomaterials* **2014**, *35* (18), 5006–5015.

(39) Zhang, Z. H.; Yin, L. C.; Tu, C. L.; Song, Z. Y.; Zhang, Y. F.; Xu, Y. X.; Tong, R.; Zhou, Q.; Ren, J.; Cheng, J. J. Redox-Responsive, Core Cross-Linked Polyester Micelles. *ACS Macro Lett.* **2013**, *2* (1), 40–44.

(40) Zhang, R. J.; Zheng, N.; Song, Z. Y.; Yin, L. C.; Cheng, J. J. The effect of side-chain functionality and hydrophobicity on the gene delivery capabilities of cationic helical polypeptides. *Biomaterials* **2014**, *35* (10), 3443–3454.

(41) Uckun, F. M.; Qazi, S.; Cheng, J. J. Targeting leukemic stem cells with multifunctional bioactive polypeptide nanoparticles. *Future Oncol.* **2015**, *11* (8), 1149–1152.

(42) Zheng, N.; Song, Z. Y.; Liu, Y.; Zhang, R. J.; Zhang, R. Y.; Yao, C.; Uckun, F. M.; Yin, L. C.; Cheng, J. J. Redox-responsive, reversibly-crosslinked thiolated cationic helical polypeptides for efficient siRNA encapsulation and delivery. *J. Controlled Release* **2015**, *205*, 231–239.

(43) Lu, H.; Wang, J.; Bai, Y. G.; Lang, J. W.; Liu, S. Y.; Lin, Y.; Cheng, J. J. Ionic polypeptides with unusual helical stability. *Nat. Commun.* **2011**, *2*, 206.

(44) Gerecht, S.; Burdick, J. A.; Ferreira, L. S.; Townsend, S. A.; Langer, R.; Vunjak-Novakovic, G. Hyaluronic acid hydrogel for controlled self-renewal and differentiation of human embryonic stem cells. *Proc. Natl. Acad. Sci. U. S. A.* **2007**, *104* (27), 11298–11303.

(45) Lu, H.; Wang, J.; Bai, Y. G.; Lang, J. W.; Liu, S. Y.; Lin, Y.; Cheng, J. J. Ionic polypeptides with unusual helical stability. *Nat. Commun.* **2011**, *2*, 206.

(46) Bang, E. K.; Gasparini, G.; Molinard, G.; Roux, A.; Sakai, N.; Matile, S. Substrate-Initiated Synthesis of Cell-Penetrating Poly-(disulfide)s. *J. Am. Chem. Soc.* **2013**, *135* (6), 2088–2091.

(47) Smolarsky, M.; Teitelbaum, D.; Sela, M.; Gitler, C. A simple fluorescent method to determine complement-mediated liposome immune lysis. *J. Immunol. Methods* **1977**, *15* (3), 255–65.

(48) Khalil, I. A.; Kogure, K.; Akita, H.; Harashima, H. Uptake pathways and subsequent intracellular trafficking in nonviral gene delivery. *Pharmacol. Rev.* **2006**, *58* (1), 32–45.

(49) Gratton, S. E. A.; Ropp, P. A.; Pohlhaus, P. D.; Luft, J. C.; Madden, V. J.; Napier, M. E.; DeSimone, J. M. The effect of particle design on cellular internalization pathways. *Proc. Natl. Acad. Sci. U. S. A.* **2008**, *105* (33), 11613–11618.

(50) Kneipp, J.; Kneipp, H.; Wittig, B.; Kneipp, K. One-and two-photon excited optical pH probing for cells using surface-enhanced Raman and hyper-Raman nanosensors. *Nano Lett.* **2007**, *7* (9), 2819–2823.

(51) Mislick, K. A.; Baldeschwieler, J. D. Evidence for the role of proteoglycans in cation-mediated gene transfer. *Proc. Natl. Acad. Sci. U. S. A.* **1996**, *93* (22), 12349–12354.

(52) Akinc, A.; Thomas, M.; Klibanov, A. M.; Langer, R. Exploring polyethylenimine-mediated DNA transfection and the proton sponge hypothesis. *J. Gene Med.* **2005**, *7* (5), 657–63.

(53) Sonawane, N. D.; Szoka, F. C.; Verkman, A. S. Chloride accumulation and swelling in endosomes enhances DNA transfer by polyamine-DNA polyplexes. *J. Biol. Chem.* **2003**, *278* (45), 44826–44831.